

Energy Management and Wake-up for IoT Networks Powered by Energy Harvesting

David E. Ruíz-Guirola, *Graduate Student Member, IEEE*, Samuel Montejo-Sánchez, *Senior Member, IEEE*, Israel Leyva-Mayorga, *Member, IEEE*, Zhu Han, *Fellow, IEEE*, Petar Popovski, *Fellow, IEEE*, and Onel L. A. López, *Senior Member, IEEE*

Abstract—The rapid growth of the Internet of Things (IoT) presents sustainability challenges such as increased maintenance requirements and overall higher energy consumption. This motivates self-sustainable IoT ecosystems based on Energy Harvesting (EH). This paper treats IoT deployments in which IoT devices (IoTDs) rely solely on EH to sense and transmit information about events/alarms to a base station (BS). The objective is to effectively manage the duty cycling of the IoTDs to prolong battery life and maximize the relevant data sent to the BS. The BS can also wake up specific IoTDs if extra information about an event is needed upon initial detection. We propose a K-nearest neighbors (KNN)-based duty cycling management to optimize energy efficiency and detection accuracy by considering spatial correlations among IoTDs' activity and their EH process. We evaluate machine learning approaches, including reinforcement learning (RL) and decision transformers (DT), to maximize information captured from events while managing energy consumption. Significant improvements over the state-of-the-art approaches are obtained in terms of energy saving by all three proposals, KNN, RL, and DT. Moreover, the RL-based solution approaches the performance of a genie-aided benchmark as the number of IoTDs increases.

Index Terms—Duty cycling, energy harvesting, energy management, Internet of Things, K-nearest neighbors, wake-up.

I. INTRODUCTION

Achieving sustainable development in today's society requires technological solutions that effectively balance economic growth, social equity, and environmental integrity [1]. These solutions must optimize resource management, improve access to essential services like healthcare and education, and minimize environmental impacts through energy-efficient practices and pollution monitoring. The Internet of Things (IoT) plays a pivotal role in this context by enabling connectivity across a wide range of applications, including mobility, safety, environmental monitoring, and resource management, to name a few [2]. Nevertheless, ensuring sustainability and autonomy in IoT systems demands a reduction in dependency on external power sources. Energy harvesting (EH) emerges as a solution, targeting self-sustainability, in which the average energy consumed over a given period is offset by the battery level and the energy harvested during the same period [3].

Despite fluctuations in consumption and EH rates, a well-designed system can achieve long-term self-sustainability, eliminating the need for recharging or manual battery replacement and supporting sustained energy autonomy [3].

Emerging network architectures increasingly emphasize sustainability, particularly given the expected ultra-dense deployment of IoT devices (IoTDs). This vision necessitates both reducing energy consumption and efficient resource allocation to maintain scalability and reliability [1]. Techniques such as wake-up receiver (WuR) and discontinuous reception (DRX) can help in this regard. WuR, for example, can potentially save up to 1,000 times the energy consumed by the main radio frequency interface (RFI), allowing IoTDs to transition to a “sleep” state while the WuR remains active [4]. This allows for on-demand operation, where the main RFI consumes energy only during communication [5]. However, configuring DRX and WuRs remains challenging due to the irregular traffic patterns in IoT networks [4]. Additionally, in self-sustainable scenarios where IoT devices rely solely on ambient EH, fluctuating energy availability poses a risk to their ability to recharge and maintain continuous operation [3]. These uncertainties complicate the design of effective energy management and duty-cycling strategies, both essential for ensuring long-term network scalability and functionality. Thus, it becomes vital to develop energy-aware mechanisms that dynamically adapt IoTDs' operation modes (e.g., “sleep”, “idle”, and “sensing”), thereby ensuring sustainable operation throughout the network's lifetime [1].

In several IoT scenarios, a base station (BS) acts as a gateway for a group of IoTDs aiming to sense/detect events or alarms. These IoTDs are deployed to identify event triggers, playing a crucial role in applications such as motion/fire detection, environmental/agricultural monitoring and remote healthcare. These applications require real-time monitoring and immediate responses to changes in the environment or conditions, as outlined in Table I. The IoTDs must meet the specific requirements of their target applications, ensuring reliable performance and long-term sustainability. Their deployment and management are thus essential for enhancing energy efficiency, safety, and sustainability across various sectors. However, as the number of deployed IoTDs increases, so do the challenges related to coordination, scalability, and energy efficiency, highlighting the need for intelligent coordination strategies and adaptive, energy-aware mechanisms [10].

This motivates the development of novel frameworks addressing energy-efficient and sustainable operation in low-power IoT networks, particularly under event-driven (ED)

David E. Ruíz-Guirola and Onel L. A. López are with the Centre for Wireless Communications, University of Oulu, Finland. {David.RuizGuirola, Onel.AlcarazLopez}@oulu.fi. Samuel Montejo-Sánchez is with the Instituto Universitario de Investigación y Desarrollo Tecnológico, Universidad Tecnológica Metropolitana, Santiago, Chile. {smontejo@utem.cl}. Israel Leyva-Mayorga and Petar Popovski are with Department of Electronic Systems, Aalborg University, Aalborg, Denmark. {ilm, petarp}@es.aau.dk. Zhu Han is with the Department of Electrical and Computer Engineering, University of Houston, Houston TX, USA. {zhan2@central.uh.edu}.

TABLE I
APPLICATIONS/EXAMPLES OF LOW-POWER IOT EVENT-TRIGGERED TRAFFIC SCENARIOS

Application	Example	Distinctive features	Typical sensors	Commun Range	Density	Ref.
Motion detection	Smart home security	Binary (motion/no motion) real-time detection, limited range and angle detection	Passive infrared sensors	Short/Medium	Low/Medium	[6]
Fire alarm system	Building safety	High sensitivity, battery backup, placed on enclosed areas	Smoke detectors, heat sensors	Short	Medium/High	[7]
Environmental monitoring	Air quality	High durability and scalability	CO ₂ , NO ₂ , air quality sensors	Medium/Long	Low/Medium	[8]
Agricultural monitoring	Smart irrigation systems	Wireless control, weather resistance, automated systems	Soil moisture, temperature sensors	Medium/Long	Low	[8]
Health monitoring	Remote patient monitoring	Wearable sensors, secure data, real-time analytics	Heart rate, glucose sensors	Short	Medium/High	[9]

traffic and energy constraints. Next, we review the state-of-the-art approaches and introduce our solution to these challenges.

A. State-of-the-Art

Notably, the strategic deployment of IoTs based on spatial correlation information can improve coverage, minimize blind spots, and optimize data transmission, increasing energy efficiency [11]. Tools like Voronoi diagrams [12] and clustering [13] have been helpful for this. For instance, the authors in [14] propose a novel channel scheduling method by leveraging clustering-based techniques, and the spatial correlation between the device's activation. However, these tools alone cannot capture the sporadic traffic patterns of IoTs [15]. To address this, recent studies have combined them with machine learning (ML) to characterize network performance, considering the spatial deployment correlation between the IoTs generating the traffic [13]. Additionally, recent advances in transformers present a promising advancement for IoT, offering superior sequential modeling capabilities and scalability [16]. Their integration with reinforcement learning (RL) enhances decision-making in resource-constrained environments like edge computing [17], improving energy efficiency in IoT networks.

ML techniques can facilitate the identification of IoT behavior patterns, enabling the implementation of energy-saving strategies such as sleep modes. Long-short term memory (LSTM)-based algorithms for learning traffic profiles, energy availability, and power consumption dynamics are presented in [4], lightening the computation/prediction-related tasks at low-power IoTs. In particular, novel deep RL schemes are proposed in [18] to manage advanced sleep modes, where the BS sequentially determines the duration of the "sleep" state. Furthermore, in [19], support vector machines (SVM), linear regression (LR), and neural networks (NN) are used to predict power consumption in smart grids, achieving up to 84% accuracy. Similarly, [20] employs a combination of decentralized and centralized RL to allocate spreading factor and transmission power, achieving significant improvements in network-level throughput and energy consumption, particularly in large and congested networks. Meanwhile, in [21], almost an 80% improvement in the performance of EH solutions for sustainable IoT systems is achieved by using RL, significantly reducing the energy consumption of IoTs. Furthermore, EH efficiency is optimized in [22] by estimating the optimal location of non-static IoTs using techniques such as K-nearest neighbors (KNN) and random forest.

Despite previous IoT-related research projects, challenges like scalability, resource efficiency, and energy efficiency persist in effectively implementing correlation-based strategies [10]. Sustainable IoT development requires a holistic approach integrated with energy-efficient technologies, optimized resource allocation strategies, and ML-based solutions. Notably, research is missing on ML-based methods for adjusting WuR and duty cycling parameters in self-sustaining IoT networks, constituting an important research gap for further increasing energy efficiency that we have been exploring recently. Our preliminary work [23] focuses on managing IoT energy consumption and EH capabilities, extending the battery life of IoTs, and addressing low-energy availability. Therein, we considered the scenario where the IoTs gather ambient energy and monitor events and alarms while in the sensing state, and proposed a KNN-based duty cycling configuration. Additionally, a wake-up method was used to minimize the mean energy consumption of the IoTs while considering the spatial correlations of their activities and a minimum information threshold required by the BS from events/alarms. The KNN-based configuration proposed in [23] showed improvement in energy saving and performance with up to 11 times less misdetection probability and a 50% decrease in energy consumption. However, while a fixed, predetermined information threshold may be practical for a specific setup, it is often impractical in broader contexts, as different IoT deployments face unique coverage and optimization challenges that require tailored solutions. Furthermore, it does not account for the inherent fluctuations and variability in the EH process, which could impact its effectiveness in real-world scenarios.

B. Contributions & Organization of this work

In this paper, we build upon [23], using the framework and wake-up method proposed therein to maximize the amount of information the BS regarding events/alarms, rather than focusing solely on minimizing energy consumption for a pre-determined minimum amount of information. By doing this, this work establishes a comprehensive framework balancing the information collected and the energy consumption required to achieve it, thus enhancing the overall energy efficiency and reliability of IoT networks in diverse applications. Table II summarizes the main features of the proposed solution and the state-of-the-art proposals.

The contributions of this paper are summarized as follows:

TABLE II
BRIEF SUMMARY: STATE-OF-THE-ART VS. OUR PROPOSAL

Ref.	WuR	EH	Goal	Focus	Tools
[4]	✓	✗	Minimize idle listening	Traffic-based WuR control	LSTM
[14]	✗	✗	Reduce redundant channel access	Channel scheduling	Clustering
[18]	✗	✗	Optimize sleep mode to save energy	Dynamic duty cycling	Deep RL
[19]	✗	✗	Optimize resource allocation	Power prediction	NN, LR, SVM
[20]	✗	✗	Optimize adaptive resource control	Spreading factor and transmission power	RL
[21]	✗	✓	Efficient EH	EH strategy	RL
[22]	✗	✓	Maximize EH collection	Node placement for EH	KNN, clustering
[23]	✓	✓	Optimize duty cycling	Spatially aware duty cycling	KNN
Our work	✓	✓	Achieve self-sustainability and info gain	Optimize jointly duty cycling, WuR, and ED	RL + KNN + clustering

- We introduce a BS-controlled duty-cycling scheme that combines KNN with Voronoi-diagram analysis to dynamically determine, for each event, the minimum data each IoTD must report to maintain efficient operation, in contrast to the static configurations used in [23]. This approach considers energy efficiency while learning the spatial correlations among IoTDs, enabling more intelligent scheduling of sensing and transmission activities.
- We propose advanced RL-based approaches, including Q -learning and decision transformer (DT), to optimize duty cycling and wake-up methods. These methods enable dynamic adaptation to varying network conditions, traffic patterns, and energy availability, making them well-suited for self-sustaining IoT environments.
- We show that the proposed KNN and RL-based configurations achieve significant performance improvements, *e.g.*, up to 4.5 times more information received per event and a 23% decrease in energy consumption compared to a random duty cycling baseline.

The rest of the paper is organized as follows. Section II presents the system model, including the models of EH, power consumption, and the influence of events on the IoTDs. Section III describes the battery state evolution, while Section IV shows the wake-up method and the IoTD transition probabilities. Section V outlines the optimization problem for the duty cycling and wake-up setup, and presents solutions based on heuristics, Voronoi diagrams, and ML. The effectiveness of the proposed methods is evaluated through numerical simulations in Section VI. Finally, we conclude the paper in Section VII.

Notation: $(\cdot)^T$ represents the transpose of a vector/matrix. Let $\mathbf{1}$ denote a row vector of ones, $\mathbf{1}_0(\cdot)$ represent the indicator function, while $\lceil \cdot \rceil$ the ceiling function and $\beta_x(\cdot, \cdot)$ the regularized incomplete beta function. Moreover, we use **bold** capital/lowercase formatting to refer to matrices/vectors.

II. SYSTEM MODEL

We consider the coverage area of a BS that serves as the gateway for a set \mathcal{N} of N IoTDs with EH capabilities as depicted in Fig. 1. Moreover, the time is slotted into

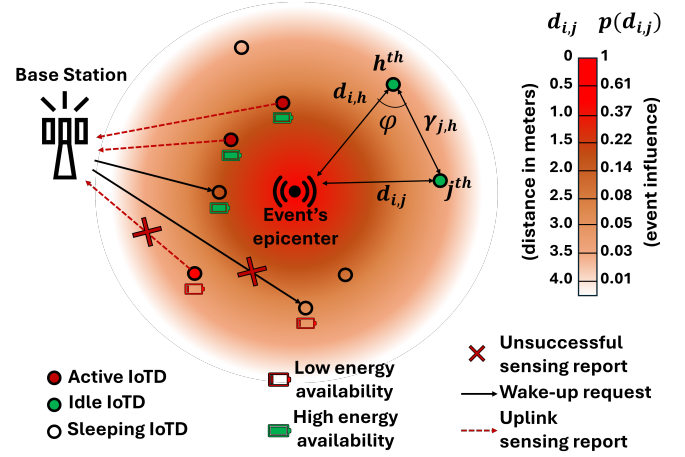


Fig. 1. Illustration of an IoT network where the BS collects information from various IoTDs that rely on EH to remain operational. The impact of an event on the surrounding IoTDs is modeled through a probability activation function that decays with the distance from the event epicenter to the IoTDs. The BS may wake-up certain IoTDs with the hope they can provide more information about a sensed event.

transmission time intervals (TTIs) with duration τ . We assume that the coordinator knows the position of each IoTD and that the epicenter of each event follows a two-dimensional uniform random distribution. Events occur independently in each TTI with probability α [4].

To describe the operation of an IoTD, let us consider four main modules, as depicted in Fig. 2. The main RFI handles conventional data exchange with other IoTDs or the BS; the sensor detects event occurrences; the EH module harvests ambient energy to sustain operation; and the WuR module includes a low-power radio interface to detect wake-up signals and activate the main radio when needed. An IoTD j can operate in four different states $S^{(j)} \in \mathcal{S} = \{S_1, S_2, S_3, S_4\}$:

- 1) “idle” state, S_1 , wherein it is waiting to be triggered by an event;
- 2) “active” state, S_2 , wherein the IoTD is triggered by an event and thus aims to send the information to the BS;
- 3) “transmission” state, S_3 , wherein it is sending the information to the BS through the main RFI; and
- 4) “sleep” state, S_4 , wherein it is staying at a low-power consumption state with only the WuR operational, while the main RFI and sensor modules are turned off.

The WuR allows the BS to trigger the IoTD when additional information is needed, ensuring availability even during state S_4 . IoTDs can harvest energy whenever it is available, regardless of their operational state. We denote $P_{m,n}^{(j)}$ as the transition probability for IoTD j from a state S_m into a state S_n . The states and their transition probabilities are described through a discrete-time Markov process, as shown in Fig. 3.

A. Event Sensing and Information Level

We define $p(d_{i,j})$ as the sensing function for an IoTD $j \in \mathcal{N}$ in the sensing state S_1 . This function represents the impact of the i^{th} event with epicenter at (x_i, y_i) on the j^{th} IoTD, within the network area $\xi \subset \mathbb{R}^2$. Here, $d_{i,j}$ indicates the distance between the epicenter of the i^{th} event and the j^{th} IoTD. Note that, $p(d_{i,j}) \rightarrow (0, 1]$ is non-increasing, modeling

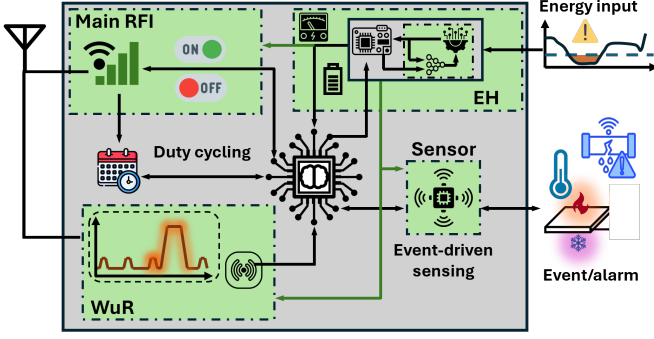


Fig. 2. Illustration of an IoTD architecture equipped with WuR and EH capabilities, showing its four main modules: main RFI, WuR, sensor, and EH unit. The EH circuit powers the other modules.

a decaying influence of events as the distance $d_{i,j}$ increases. Fig. 1 illustrates an example of the influence of an event epicenter on the surrounding IoTDs and note that the spatial activity correlation depends on $p(d_{i,j})$. Active devices transmit packets to the BS, managing all information exchanges within its cell [4], all with the same transmission power. In state S_2 (“active”), devices generate traffic, while no traffic is generated in the other states.

Active IoTDs send information about the detected event. In this study, we model the amount of information sent by each IoTD in state S_2 as

$$I_{i,j} = \Psi p(d_{i,j}), \quad (1)$$

where $\Psi > 0$ constitutes the maximum amount of information that an IoTD can capture from an event. The BS gathers the information reported by the IoTDs. Specifically the information about the i^{th} event at the BS is given by

$$I_i = g(\{I_{i,j}\}_{\forall j: S(j)=S_2}). \quad (2)$$

Here, $I_{i,j} = 0$ for those IoTDs with insufficient energy to transmit information or for those where the event is outside the sensing range. Therefore, if no IoTD detects the event, then $I_i = 0$. Meanwhile, the function g determines the amount of information that the BS can collect from the IoTDs triggered by events, and there may be several formulations for it. This function accounts for the correlation between the information collected by different devices from the same event.

One potential function g is $\max_j(I_{i,j})$, which is commonly used in temperature or motion sensing applications. This function is useful when the highest value, corresponding to the device closest to the event epicenter, represents the critical or most relevant information, and other values are considered redundant or less important. Another potential function is a sum with saturation, *i.e.*,

$$I_i = \min\left(\sum_{j=1}^N I_{i,j}, \Psi\right). \quad (3)$$

This function applies to situations where the effect of observations increases to a certain point and then levels off. Specifically, scenarios such as pollution sensors where the health risks increase as the concentration of pollutants rises, but they level off once a maximum threshold is reached. Similarly, in acoustic sensors, where noise impact on health increases with intensity but eventually saturates. Additionally,

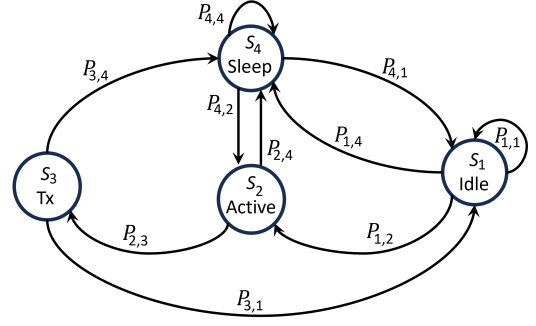


Fig. 3. The IoTD's operation states are modeled as a four-state discrete-time Markov chain.

in data collection, bandwidth usage increases as more data is transmitted, but it reaches a point of saturation at the network's maximum capacity. Here, the piecewise function can cap the total information collected to prevent overloading the BS. Finally, controlling the number of active IoTDs may be necessary to conserve energy, particularly in battery-powered devices, and this approach also helps in managing that.

III. ENERGY MODELLING

This section presents a discrete-time model of battery dynamics powered by ambient EH. We characterize the energy consumption and EH processes, followed by a Markov-based framework to capture battery state evolution and evaluate the probability of sufficient energy availability for operation.

A. Energy Consumption and Harvesting Model

We assume discrete EH and storage for device batteries, which have maximum capacity E_{\max} . Additionally, transmitting in state S_2 results in a depletion of E_{Tx} units, while monitoring events in state S_1 consumes E_{idle} units per TTI, and the WuR in state S_2 consumes E_{WuR} , as depicted in Fig. 4. We assume that if the battery level (B) of an IoTD at the moment of transmission is lower than the level needed to transmit or perform event monitoring, the battery is depleted and the action is unsuccessful.

In this paper, we adopt a simplified model based on [4], where the mean energy consumption (\bar{C}) is calculated based on the energy consumption of battery units (C_m) for every state S_m . This is summarized as the mean energy units consumed per IoTD per TTI and written as

$$\bar{C} = \frac{1}{N} \sum_{j=1}^N \sum_{m=1}^4 \Pr(S^{(j)} = S_m) C_m. \quad (4)$$

At each TTI, we also model the energy harvested by the IoTDs by using N modulated Poisson processes (MPPs), one for each IoTD. Specifically, a Poisson process is used to model the occurrence of energy arrivals within a certain time interval. The energy arrival duration, *i.e.*, the time duration in case the energy source remains active, is modeled with an exponential distribution with mean μ_j . At each TTI, at most one energy arrival occurs from an energy source. In that case, the energy source can be considered as active or inactive within one time slot as shown in Fig. 4. By defining $\lambda_j = 1/\mu_j$, the

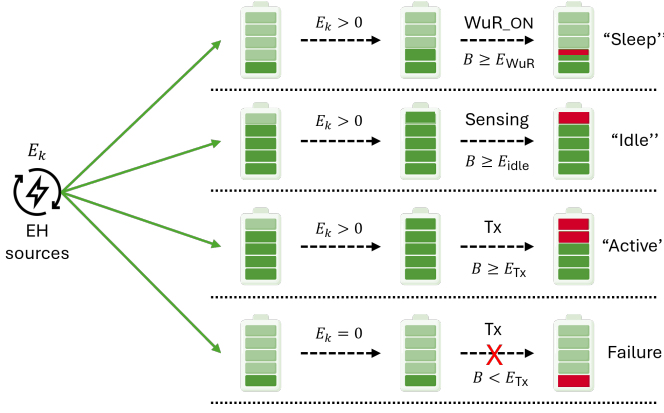


Fig. 4. Illustration of the battery level evolution by considering the energy consumption and EH models. Transmission (Tx) results in the highest energy depletion, while “sleep” is a low-energy consumption state. The sensing results in a depletion smaller than Tx but greater than a “sleep” state. IoTds that do not have sufficient energy to carry out these actions will fail.

probability of the energy source being active within one TTI can be expressed as

$$p_j = \lambda_j \tau \exp(-\lambda_j \tau). \quad (5)$$

B. Battery State Evolution

The probability that an IoTd has sufficient energy in the battery to perform transmission or sensing depends on the energy harvested at each TTI plus the initial battery level and previous actions the IoTd performs. To calculate this probability, we can use a discrete-time Markov chain to model the battery level over time. We define several states for the battery level, while transitions occur based on the EH process and battery consumption operations.

Let us define E_B as the units of energy an IoTd can harvest when the energy source is active. Then, following MPP, harvesting E_B units of energy occurs with probability $\exp(-\lambda_j)$. We formulate a discrete Markov chain with states representing the battery level (from 0 to E_{\max} units), where E_{\max} is the maximum capacity of the IoTd battery. Let us denote the states of the battery level as follows:

- State 0: Battery level is 0 units;
- State 1: Battery level is E_λ units;
- State 2: Battery level is $2E_\lambda$ units;
- ...
- State $\lceil E_{\max}/E_\lambda \rceil$: Battery level is E_{\max} units;

where $E_\lambda = E_B \exp(-\lambda_j)$. We calculate the transition probabilities between these states based on the EH process and battery consumption operations. Assuming a steady state, the state arrival rate equals the state departure rate. Therefore, we can use the fact that $\sum_{b=0}^{\lceil E_{\max}/E_\lambda \rceil} b = 1$, where b is the steady B state probability, to solve $\mathbf{R}_{B,B} \times \mathbf{b} = \mathbf{c}$, where $\mathbf{c} = [1, 1, \dots, 1]^T$, $\mathbf{b} = [b_0, b_1, \dots, b_{\lceil E_{\max}/E_\lambda \rceil}]^T$, and

$$\mathbf{R}_{B,B} = \begin{pmatrix} R_{0,0} & R_{0,1} & \cdots & R_{0,\lceil \frac{E_{\max}}{E_\lambda} \rceil} \\ R_{1,0} & R_{1,1} & \cdots & R_{1,\lceil \frac{E_{\max}}{E_\lambda} \rceil} \\ \vdots & \vdots & \ddots & \vdots \\ R_{\lceil \frac{E_{\max}}{E_\lambda} \rceil,0} & R_{\lceil \frac{E_{\max}}{E_\lambda} \rceil,1} & \cdots & R_{\lceil \frac{E_{\max}}{E_\lambda} \rceil,\lceil \frac{E_{\max}}{E_\lambda} \rceil} \\ 1 & 1 & \cdots & 1 \end{pmatrix} \quad (6)$$

is the transition matrix. Herein, $R_{k,l}$ represents the transition probability from a battery state $B = k$ to a battery state $B = l$.

Now, we proceed to find the probability of being in a state with sufficient battery to perform the operation that needs E_{Tx} units, i.e., $\Pr(B \geq E_{Tx})$. Note that IoTd j goes to state S_2 with probability $P_{1,2}^{(j)} + P_{4,2}^{(j)}$. While in S_2 , we need to check whether the IoTd has sufficient energy to transmit the sensed information. Exploiting the previously presented Markov chain for the battery state evolution, we obtain

$$\Pr(B^{(j)} \geq E_{Tx}) = \sum_{B=E_{Tx}}^{\lceil E_{\max}/E_\lambda \rceil} \binom{B}{E_{Tx}} \frac{(P_{1,2}^{(j)} + P_{4,2}^{(j)})^{E_{Tx}}}{(1 - P_{1,2}^{(j)} - P_{4,2}^{(j)})^{E_{Tx}-B}}, \quad (7)$$

where the binomial coefficient represents the number of ways the IoTd can accumulate enough energy to transmit E_{Tx} , and the transition probabilities account for the activation probabilities that lead or not to consuming E_{Tx} . This expression has a semi-closed form using the regularized incomplete beta function, $\beta_{1-P_{1,2}^{(j)}-P_{4,2}^{(j)}}(E_{Tx}+1, E_{\max}+1)$, with parameters $E_{Tx}+1$ and $E_{\max}+1$ [24]. We can similarly calculate $\Pr(B^{(j)} \geq E_{idle})$, i.e., the probability that the IoTd can sense in state S_1 .

IV. ON-DEMAND WAKE-UP AND TRANSITION PROBABILITIES

We assume the IoTds are equipped with WuR modules to detect requests from the BS to either enter the “active” state (S_2) or switch between states. The WuR module allows IoTds with low-energy availability to remain in state S_4 while ensuring their availability to provide additional information to the BS when required (with probability $P_{4,2}^{(j)}$). The BS may try to wake up certain IoTds in state S_4 to sense potential events based on information received from other IoTds and their spatial correlation. However, this might not always be possible because each IoTd j with low-energy availability stays in state S_4 (with probability $P_{4,4}^{(j)}$) and harvests energy for future events. Meanwhile, IoTds in state S_4 with high-energy availability may be authorized by the BS to move from state S_4 to S_1 to monitor potential events. Then, the transitions between states for IoTd j can occur as follows.

- A transition from state S_4 to S_1 occurs during the ON time of the duty cycling, t_{on} , then

$$P_{4,1}^{(j)} = t_{on}/t_{DRX}, \quad (8)$$

where t_{DRX} is for the time between consecutive ON states (S_1). Otherwise, the IoTd stays in state S_4 with probability $P_{4,4}^{(j)} = 1 - P_{4,1}^{(j)} - P_{4,2}^{(j)}$. Note that t_{on} and t_{DRX} are integer multiples of τ .

- A transition from state S_4 to S_2 occurs when the BS determines that additional information about an event is needed. Based on the current information I_i , the learned spatial correlation, and the probability $\Pr(B^{(j)} \geq E_{Tx})$, the BS sends a wake-up request. Upon receiving it via the WuR, the IoTd transitions to state S_2 , activating both its sensor and main RFI modules. To determine the transition probability, we use the conditional probability $\Pr(S^{(j)} = S_3 | S^{(h)} =$

S_3), which represents the probability that an IoTD j is in state S_3 given that another IoTD h is in state S_3 . Then,

$$P_{4,2}^{(j)} = \max \Pr(S^{(j)} = S_3 | S^{(h)} = S_3), \quad (9)$$

wherein the maximum value captures the highest activation probability when an event is detected. Herein, $\Pr(S^{(j)} = S_3 | S^{(h)} = S_3)$ is determined by the spatial correlation between IoTD j and each IoTD h in state S_3 . We calculate $\Pr(S^{(j)} = S_3 | S^{(h)} = S_3)$ using the cosine rule as

$$d_{i,j}^2 = d_{i,h}^2 + \gamma_{j,h}^2 - 2d_{i,h}\gamma_{j,h}\cos\varphi, \quad (10)$$

where $\gamma_{j,h}$ denotes the distance between both devices and φ is the angle between vectors $\vec{d}_{i,h}$ and $\vec{\gamma}_{j,h}$, as depicted in Fig. 1. Then,

$$\Pr(S^{(j)} = S_3 | S^{(h)} = S_3) = p\left(\sqrt{d_{i,h}^2 + \gamma_{j,h}^2 - 2d_{i,h}\gamma_{j,h}\cos\varphi}\right), \quad (11)$$

where $d_{i,h}$ and $\gamma_{j,h}$ are known, and φ has a uniform distribution in $[0, 2\pi)$.

- A transition from state S_1 to S_2 for an event (i) occurs with probability $P_{1,2}^{(j)} = \alpha p(d_{i,j})$. Otherwise, the IoTD stays in state S_1 with probability

$$P_{1,1}^{(j)} = \sum_{i=\tau}^{t_{on}} (1 - \alpha)^i \frac{t_{on} - i}{t_{DRX} - i}, \quad (12)$$

while transits from state S_1 to S_4 with probability $P_{1,4}^{(j)} = 1 - P_{1,1}^{(j)} - P_{1,2}^{(j)}$.

- A transition from state S_2 to S_3 occurs when B is enough to transmit, thus $P_{2,3}^{(j)} = \Pr(B \geq E_{Tx})$, while the device transits from state S_2 to S_4 with probability $P_{2,4}^{(j)} = 1 - P_{2,3}^{(j)}$.
- A transition from state S_3 to S_1 occurs with probability

$$P_{3,1}^{(j)} = \sum_{i=\tau}^{t_{on}} \frac{t_{on} - i}{t_{DRX} - i}, \quad (13)$$

Otherwise, the transition is to state S_4 with probability $P_{3,4}^{(j)} = 1 - P_{3,1}^{(j)}$.

V. OPTIMIZATION FRAMEWORK

An IoTD duty cycling and wake-up management policy controlled by the BS is referred to as $\delta(k) = [\delta_1(k), \delta_2(k), \dots, \delta_N(k)]$ for each TTI $k \in [0, K]$, where K represents the total number of TTIs during analysis. At each TTI k , $\delta(k)$ designates which IoTDs will be in S_1 , waiting to be triggered or woken up from S_4 to S_2 (designated by 1), and which IoTDs will remain in S_4 (designated by 0). Here, $\delta(k)$ must take into account $\Pr(B^{(j)} \geq E_{idle})$ and $\Pr(B^{(j)} \geq E_{Tx})$ due to the energy arrivals at random times and the finite battery storage capacity. This approach helps save power by not prompting an IoTD with low energy levels to wake up and transmit information. Such an action would otherwise drain the battery, preventing the IoTD from transferring the information detected.

In a long time interval (*i.e.*, large K), maximizing the information about event I_i and minimizing the probability of missing events mainly depends on the energy available in the IoTDs batteries. Reducing energy consumption means having

a greater density of IoTDs with high energy availability for event sensing and reporting. However, we need to carefully balance energy savings to ensure high energy availability when needed, while also keeping a sufficient number of IoTDs sensing and reporting to cover a large area and prevent events from going undetected. This, in turn, leads to fewer blind spots where events may go unnoticed, consequently decreasing the misdetection probability. In addition, it increases the probability that the IoTD closest to the event has high energy availability, increasing the received information about the event.

The proposed optimization problem is stated as

$$P1 : \max_{\delta(k)} \frac{1}{\alpha K} \sum_{\forall i} I_i. \quad (14)$$

Here, we use the expected number of events, αK , as a normalization factor instead of the exact number of events, since the latter cannot be known, while α can be inferred from historical data. Note that false alarm reports do not contribute to (14) as they don't lead to a positive $I_{i,j}$ for any j . In addition, IoTDs with limited energy availability cannot report, so ensuring high energy availability is a crucial condition to maximize information in (14).

Inherently, solving problem P1 in (14) entails enhancing battery lifetime within the network. This is because maximizing the information about events necessitates maintaining the devices' battery levels above the threshold required for transmission. Only these devices can transmit event information. Therefore, by maximizing the received information the energy efficiency of the network is also promoted.

Optimization methods to solve this problem can be computationally intensive and time-consuming. The complexity of solving the problem increases significantly as the number of IoTDs grows [11]. Specifically, solving (14) would require a detailed analysis of the system's evolution over time and the IoTDs' energy availability, which is not practical. In light of this, we aim to propose heuristic and data-driven approaches to address the issue in a more computationally efficient way.

A. Heuristic & KNN-based Duty Cycling

In our recent conference work [23], we established a minimum expected information level per event, denoted as I_{min} , while aiming to minimize the average energy consumption, denoted as \bar{C} . Our goal here is to solve P1 (14) by reframing the heuristic approximations based on exhaustive search and KNN presented in [23], which is not straightforward. The main challenge lies in the limitations of the adjusted duty cycling and KNN approaches when applied to P1 (14). Specifically, these methods lack effective mechanisms to control and balance the trade-off necessary to maintain the IoTDs with high energy availability. To tackle the issue, we first determine a realistic target for $\frac{1}{\alpha K} \sum_{\forall i} I_i$ in (14) based on the spatial deployment of the IoTDs. We then calculate the minimum energy required to achieve this information level using the the adjusted duty cycling and KNN-based heuristic methods. Our objective is to prevent the depletion of the IoTDs' energy reserves while ensuring that the desired realistic information level is attained following event detection.

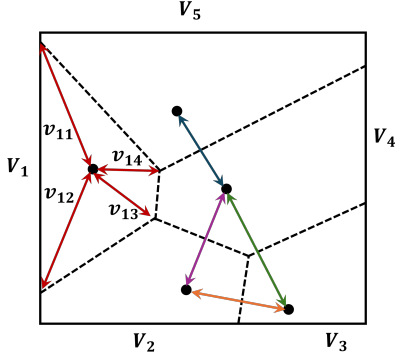


Fig. 5. Illustration of a Voronoi diagram for a grid IoT deployment with five devices (represented as black dots). The black dashed lines represent the perpendicular bisectors of the arrows that connect neighboring IoT devices, which form the Voronoi polygon corresponding to each IoT, V_j . The red arrows represent the distances to the vertices, v_j , of a Voronoi cell.

We formulate the optimization problem in P1 with the framework from [23] to minimize the energy consumption while achieving the expected information level from the events, I_{\min} , for each spatial deployment as

$$\text{P2: } \min_{\delta(k)} \bar{C} \quad (15a)$$

$$\text{s.t. } \frac{1}{\alpha K} \sum_{\forall i} I_i \geq I_{\min}. \quad (15b)$$

Herein, \bar{C} can be reformulated from (4) as

$$\bar{C} = \frac{1}{NK} \sum_{k=1}^K \sum_{j=1}^N \delta_j(k) (E_{\text{idle}} + \Pr(S^{(j)} = S_3) E_{\text{Tx}}) + \dots \\ \dots + (1 - \delta_j(k)) E_{\text{WuR}}. \quad (16)$$

We assume that state S_2 is a conditional transition state so the energy consumption in that state is neglected. Note that at each TTI k , IoTs with $\delta_j = 1$ need high energy availability for sensing/transmitting while IoTs with $\delta_j = 0$ have a low energy consumption in “sleep” state S_4 related to the WuR consumption, E_{WuR} . Therefore, proper $\delta(k)$ management is crucial at each TTI.

Here, we calculate the expected value of I_{\min} for the network deployment based on the spatial positioning of IoTs. This contrasts with [23], where this value must be given beforehand. To calculate $\mathbb{E}(I_{\min})$, we construct the Voronoi diagram for the set of N IoTs positions, as shown in Fig. 5. Each cell in the Voronoi diagram contains all points that are closer to a particular IoT than to any other device, V_j . Next, for each IoT j , we find the vertices of its Voronoi cell, $v_j = \{v_{j1}, v_{j2}, \dots, v_{j\kappa}\}$, where κ is the total number of vertices for the Voronoi cell V_j . These vertices are intersections of the perpendicular bisectors of the lines connecting the device to its neighboring devices [12]. Then, $\mathbb{E}(I_{\min})$ is calculated using the maximum of these distances across all Voronoi cells d^* as: $\mathbb{E}(I_{\min}) = p(d^*)$, where

$$d^* = \max_j \sqrt{(x_j - x_{v_j})^2 + (y_j - y_{v_j})^2}. \quad (17)$$

A particular example is the deployment of an IoT grid, for which we have

$$\mathbb{E}(I_{\min}) = p\left(\sqrt{\xi/(2N)}\right) \quad (18)$$

Here, the sensing area assigned to each IoT is a square area of side $\sqrt{\xi/N}$ and the maximum distance from the center (*i.e.*, IoT) to the side of this area is $\sqrt{\xi/(2N)}$.

Next, we outline two potential approaches to tackle the current problem using the previously calculated $\mathbb{E}(I_{\min})$.

- 1) We adjust the IoT duty cycling by an exhaustive search within t_{on} (S_1) and t_{DRX} values. The duration of t_{on} (S_1) plus “sleep” state (S_4) within a cycle constitutes the t_{DRX} value. Hereinafter, we refer to this approach as “adjusted duty cycling”.
- 2) We form clusters based on each device’s spatial placement. We create a graph structure using KNN method as follows: 1) set the assignment of IoTs to each cluster randomly, 2) calculate the distance to the neighbors, 3) identify each IoT KNN based on the distances, and 4) assign each IoT to the cluster that the majority of its KNN belong to, and 5) update centroids and repeat steps 2-5 until convergence to achieve the correct IoT assignment to each cluster [12]. The algorithm sets a maximum distance d_{max} , linked to the minimum sensing power $p(d_{\text{max}})$ set to form the clusters. The aim is to reduce the misdetection probability by limiting the sensing area controlled by the clusters. Then, we configure the duty cycling of the IoTs in each cluster. In each TTI, the IoTs within a cluster iterate a round-robin sensing in S_1 . That is, during each TTI, only one IoT is actively sensing in S_1 while the other IoTs in the cluster are in S_4 , ensuring there is always one IoT in S_1 during each TTI. In each cluster, the t_{DRX} duration for IoTs within that cluster is equal to the number of IoTs in that cluster. This proposed approach is summarized in Algorithm 1.

Notice that the first approach differs from the second one in the duty cycling configuration. Indeed, the BS wake-up request for the first approach is based on the IoT’s correlation rather than cluster-based, as in Algorithm 1. In both approaches, the BS may request more information about an event from the other IoTs in state S_4 that have a strong spatial correlation with the IoTs in state S_3 , line 7. In this way, the BS requests only the needed information using the WuR technology.

Satisfying a minimum expected information per event requires maintaining IoTs’ sensing/reporting availability. That is, maintaining the battery level of IoTs above the threshold required for transmission. Only these IoTs can transmit event information. At the same time, proper sensing cycling and wake-up strategy help to reduce energy consumption and avoid misdetections, which worsen the mean information captured per event. Herein, we ensure that the model maintains the minimum level of information that the BS requires from an event above a threshold (I_{\min}) according to the spatial deployment of the IoTs. Having access to a certain level of information from IoTs enhances the BS’s ability to effectively manage the network, respond to events, and ensure the overall reliability and performance of the IoT system. Note

Algorithm 1 KNN-based solution

```

1: Set number of clusters ( $M$ ) as  $\xi/(\pi d_{\max}^2)$ 
2: Form clusters using KNN method
3: Configure duty cycling of IoTDS according to its cluster associ-
   ation ( $t_{on} = 1$ , duty cycle = cluster size)
4: for each  $k$  do
5:   if BS receives information from “active” IoTDS then
6:      $\hat{I}_i = \max_{h:S^{(h)}=S_3} (I_{i,h})$ ,
7:     while  $\hat{I}_i < I_{\min}$  do
8:       BS sequentially activates IoTDS  $\forall j : S^{(j)} = S_4$ 
       with  $\Pr(S^{(j)} = S_3 | S^{(h)} = S_3) \geq p(d_{\max})$ ,
        $\forall h : S^{(h)} = S_3$ , one at a time in each loop,
       starting with the one with the highest value,
       while updating  $\hat{I}_i = \max_{j:S^{(j)}=S_3} (\hat{I}_i, I_{i,j})$ 
9:     end while
10:    Update  $I_i \leftarrow \hat{I}_i$ 
11:   end if
12: end for

```

that a shorter t_{DRX} decreases the misdetection probability when there is high energy availability; however, it increases the energy consumption and the risk of low energy availability. Then, balancing energy saving and sensing availability to lower the misdetection probability is paramount.

B. Reinforcement Learning-based Duty Cycling and Wake-up

Model-free RL is a method for solving decision-making problems and finding optimal solutions in dynamic environments [25]. Herein, we treat our optimization problem (14) as an RL challenge, where a conventional Q -learning algorithm can be adapted to learn the optimal policy [26]. Specifically, we consider the IoTDS deployment as the environment, while the central controller at the BS functions as the agent in a centralized learning framework. The key components of our RL framework are outlined as follows.

1) The focus is on configuring duty cycling to save energy on the devices while preventing misdetections due to events not being detected or events being detected by devices without enough energy. Specifically, let \mathcal{T} denote the system state space. The system state at TTI k , $\mathcal{T}(k)$, encompasses the status of each device (“sleep” S_3 or “idle” S_2), the received sensing power from the event denoted by the sensing function $p(d_{i,j})$, the position of the IoTDSs, and battery level. Additionally, the positions of the devices and their current thresholds are known. The state of each IoTDS at TTI k is defined as

$$\mathcal{T}(k) = \{\{\delta_j(k)\}, \{p(d_{i,j})\}, \{(x_j, y_j)\}, \{B^{(j)}\}\}_{j \in \mathcal{N}}, \quad (19)$$

where $\{p(d_{i,j})\}$ for those devices that did not report is estimated using $P_{4,2}^{(j)}$ according to (10) and (11) from the spatial correlation with the IoTDSs that did report. Given an observed state “ \mathcal{T} ”, the BS adjusts $\delta(k)$ for each device based on the reward/penalty function. The action space is thus binary, $\delta_j \in [0, 1]; \forall j \in \mathcal{N}$.

In RL, the reward function evaluates the effectiveness of the duty-cycling policy when the BS takes action in the current state. At each learning step, the system performance aligns with the desired objective [25]. Hence, a reward function

capable of enhancing energy efficiency without increasing misdetection is crucial. Therefore, the reward function is formulated as

$$r(k) = \left(1 - \frac{\delta(k)\mathbf{1}^T}{N}\right) - \alpha\mu_1\mathbf{1}_0(I_i), \quad (20)$$

where the coefficient μ_1 is a positive constant for balancing utility and cost. Additionally, the first term represents the energy efficiency factor, and the second one is the misdetection factor. Note that the indicator function in the second term imposes the error probability satisfaction level: if no misdetection occurs, then no punishment of the reward function due to any error.

2) We focus on the case that the BS might require further information about the event once is detected. Once an event is detected, the current system state $\mathcal{T}(k)$ encompasses the status of each device (“sleep” S_3 or “active” S_1), their received sensing power from the event denoted by the sensing function $p(d_{i,j})$, and information on IoTDSs’ battery level. Additionally, the current state of each device is also defined by (19). Given an observed state “ \mathcal{T} ”, the BS adjusts $\delta^*(k)$ for each device in case it needs more information about the event. The action space is thus also binary, $\delta_j^* \in [0, 1]; \forall j \in \mathcal{N}$. At this stage, the reward function is formulated as

$$r^*(k) = \mu_2 I_i - \delta^*(k)\mathbf{1}^T/N, \quad (21)$$

where μ_2 is a positive constant for balancing utility and cost, imposing a satisfaction level for I_i and punishing low information flow. Meanwhile, the second term accounts for the efficiency in waking up IoTDSs previously in S_3 .

The goal is to determine an optimal policy π^* , with $\pi^*(\mathcal{T}(k)) : \mathcal{T}(k) + \pi^* \rightarrow \mathcal{T}(k+1)$ [26], that maximizes the long-term expected discounted reward. The latter is given by

$$U_k = \sum_{i=0}^k \zeta^i r_{i+1}, \quad (22)$$

where $\zeta \in (0, 1]$ is the discount factor whose impact decreases exponentially with each state k and r_{k+1} is the reward at the next state. Note that the BS determines $\delta(k)$ whenever an action is required, ensuring that IoTDSs are free from any computational burden associated with the decision-making process beyond their predefined duty cycle. The decision-making process is handled entirely by the central BS. Furthermore, this modification is binary, resulting in negligible overhead on the control channel from the BS to the IoTDSs.

C. Decision Transformer-based Duty Cycling and Wake-up

RL approaches require significant interaction with the environment for dynamic data collection. This is particularly challenging in domains where interactions are costly, and thus training data acquisition might be limited. As a result, off-line RL has been gaining attention as a data-driven learning method that can derive policies from static datasets collected previously without interaction with the environment [17]. The offline RL setting can fully extract the optimal policy from a large amount of offline data but also needs to address the distribution discrepancy between the offline training data and the target policy. However, this makes it harder for agents

Algorithm 2 DT-based solution

- 1: **Set** initial parameters for the linear transformation model $\mathcal{W}(\cdot)$ and the weight for each episode $\phi(k)_i$
- 2: **Set** RL policy (23)
- 3: **for** each episode **do**
- 4: **Compute** attention mechanism projections (key $\phi(k)_i^{\mathcal{W}_1}$, query $\phi(k)_i^{\mathcal{W}_2}$, and value $\phi(k)_i^{\mathcal{W}_3}$), and **calculate** attention scores weights using (25)
- 5: **end for**
- 6: **Calculate** and **concatenate** outputs using (24)
- 7: **Update** state $\{\mathcal{T}(k)\}$, and the action $\{a_j(k)\}$, *i.e.*, set new values for $\delta(k+1)$
- 8: **Calculate** $\{r(k+1)\}$ and **update** parameters for DT model, $\mathcal{W}(\cdot)$ and $\phi(k)_i$

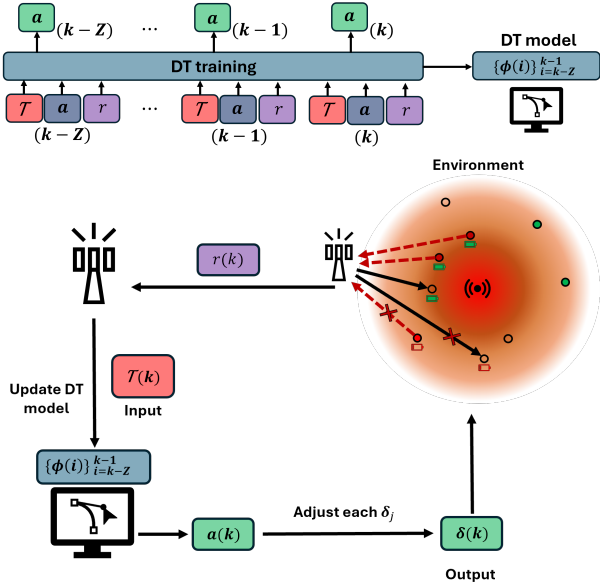


Fig. 6. Illustration of an RL-based Transformer. a) Learning process for one task of Z episodes using DT-architecture (top), and b) IoT network setup using DT-model (bottom). Note that the DT model is run at the BS.

since they cannot explore the environment or gather more feedback. In this sense, due to the sequential decision process of RL, a natural idea is to use transformers [27] as alternative architectures to improve RL methods [17]. DT considers the RL problem as a task for modeling conditional sequences and avoids traditional RL challenges, and it is adopted here. Specifically, DT is used to obtain an RL model offline and then use it to predict a decision policy online.

During DT's training process, we repeatedly sample a batch of tasks to gather experience and thus learn. For each task, we execute a sequence of Z episodes (TTIs). During optimization, we combine these episodes to optimize a single policy model and aim to maximize the discounted cumulative reward of this policy. Specifically, transformers consist of stacked self-attention layers with residual connections. Each layer of self-attention receives N embeddings $\phi(k)$, corresponding to unique input tokens with $\phi(k) = \{\{\mathcal{T}(k)\}, \{a_j(k)\}_{j \in \mathcal{N}}, \{r(k)\}\}$ representing a working memory at TTI k , according to the state $\mathcal{T}(k)$, the action $a_j(k) \sim \pi(\mathcal{T}(k))$, and the reward $r(k)$ in (20), as shown in Fig. 6a. We also have N outputs $\{\delta_j(k)\}_{j \in \mathcal{N}}$, preserving the

input dimensions.

Then, we represent each task as a linear combination of the Z working episodes, $[\phi(k-Z), \phi(k)]$, sampled as

$$\delta(k) = \sum_{i=1}^Z \psi_i \mathcal{W}(\phi(k)_i), \quad \text{with} \quad \sum_{i=1}^Z \psi_i = 1, \quad (23)$$

where $\mathcal{W}(\cdot)$ represents an arbitrary linear transformation. Moreover, ψ_i is a coefficient to indicate how relevant a particular episode is to the task representation given the set of sampled TTIs. The input is assigned via linear transformations with $\mathcal{W}(\cdot)$ to a key $\phi(k)_i^{\mathcal{W}_1}$, a query $\phi(k)_i^{\mathcal{W}_2}$, and a value $\phi(k)_i^{\mathcal{W}_3}$. The output of the self-attention layer is then given by weighting the values $\phi(k)_i^{\mathcal{W}_3}$ by the normalized dot product between the query $\phi(k)_i^{\mathcal{W}_2}$ and other keys $\phi(k)_i^{\mathcal{W}_1}$ using the softmax function [28], obtaining

$$\delta(k) = \sum_{i=1}^Z \text{softmax} \left(\langle \phi(k)_i^{\mathcal{W}_2}, \{\phi(k)_{i^*}^{\mathcal{W}_1}\} \rangle \right) \phi(k)_i^{\mathcal{W}_3}, \quad (24)$$

where

$$\text{softmax}(\langle a, \{b_{i^*}\} \rangle) = \frac{\exp(a)}{\sum_{i^*=1}^Z \exp(b_{i^*})}. \quad (25)$$

This approach allows us to attribute “credit” to the layer by creating connections between the state and return through the similarity of the query and key vectors (maximizing the dot product). This enables the model to generate a policy $\delta(k)$ based on the current state $\mathcal{T}(k)$ and the preceding Z episodes $\{\phi(k)_i\}_{i=k-Z}^{k-1}$, as shown in Fig. 6b. The proposed approach is summarized in Algorithm 2.

D. Complexity and Implementation Aspects

The adjusted duty cycling involves an exhaustive search within t_{on} and t_{DRX} . Its computational cost is $\mathcal{O}(\varrho^N)$ where ϱ is the number of possible t_{on} values multiplied by the number of possible t_{DRX} values. On the other hand, the complexity of the approach implementing KNN is bounded to $\mathcal{O}(N(N-1)/2)$. Such a worst-case complexity arises due to the distance computation to the N IoTD for each query point using a brute-force approach. However, as previously mentioned, the computation time can differ based on the utilized algorithm, occasionally reducing to $\mathcal{O}(\min\{M(N-M), (N-M)^2\})$, where M is the number of clusters [12]. Meanwhile, the complexity of the RL-based approach might vary depending on the initial values and the algorithm implementation. However, the worst-case complexity is $\mathcal{O}(N^2)$. Similarly, the computational complexity of the self-attention mechanism in transformers increases quadratically with the input sequence length (N). The exact complexity depends on the specific algorithms and how fast they converge. Notice that RL is the only one that requires online implementation or a quite large dataset at least.

Note that the policy $\delta(k)$ does not require updates at every TTI. Once the approaches are trained and/or implemented, the sensing policy remains fixed for each specific spatial deployment. Updates from the BS to the IoTDs are only necessary when an event is detected or periodically for synchronization purposes. However, these synchronization updates occur at intervals significantly longer than typical TTI durations. Furthermore, as mentioned previously, these updates

TABLE III
SIMULATION PARAMETERS

Parameter	Value	Ref.
d_{max}	4 meters	[13]
η	1	[4], [29]
Ψ	1	[4], [29]
ξ	20×20	[4], [29]*
E_{max}	100 units	[4], [30] [†]
E_{idle}	1 units	[4], [5], [30] [†]
E_{WuR}	1/14 units	[4], [5] [†]
E_{Tx}	10 units	[4], [5], [30] [†]
$p(d_{i,j})$	$e^{-\eta d_{i,j}}$	[4], [29]
N	[10, 250]	[4], [29]*

*The values of ξ and N lead to a density range $[0.025, 0.625]$ IoTds/m².

[†]Energy parameters are normalized from typical values.

are binary, resulting in negligible overhead on the control channel between the BS and the IoTds. Moreover, the learning process for each approach represents a one-time energy cost at the BS, while the resulting duty cycling and EH operations ensure sustained long-term energy efficiency at the IoTds.

VI. SIMULATIONS

We consider a 20×20 m² area with $N \in [10, 250]$. Note that $N < 10$ is not enough to cover the area, leading to many misdetection events, thus we ignore such setups. We assume an exponentially decreasing function, i.e., $p(d_{i,j}) = e^{-\eta d_{i,j}}$, with $\eta = 1$ [4], and $\Psi = 1$, related to the ideal case when $d_{i,j} = 0$. We perform 10^3 runs of Monte Carlo simulations, each having different deployments and lasting 10^4 TTIs. In addition, we assume $E_{Tx} = 10$ units while $E_{idle} = 1$ unit, $E_{WuR} = 1/14$ units, $E_{max} = 100$ units, and $p(d_{max}) = 0.018$ corresponding to $d_{max} = 4$ meters [13]. We assume IoTds performing EH with $\lambda_j = \lambda, \forall j \in \mathcal{N}$. Table III summarizes the parameters used in simulations unless explicitly stated otherwise.

We consider two benchmarks. In the first one, we let each device adopt a random duty cycling with $t_{on} \in [1, 2]$ and $t_{DRX} \in [2, 4, 8]$ for light sleep and avoiding misdetection [31]. For the second one, we adopt a genie-aided approach wherein the closest IoTd to the event epicenter always detects the event. If the closest IoTd is more than d_{max} away, then it is considered a misdetection. It is important to mention that this approach is not feasible in practice because the BS would need to know a priori which IoTd is the closest to the event epicenter to activate it using WuR. Nevertheless, this approach provides an upper bound in performance. We also evaluate the effect of the reward weights $\mu_1 \in [0.5, 20]$ and $\mu_2 \in [1, 5]$ in the RL-based approach. Specifically, μ_1 controls the trade-off between detection accuracy and energy consumption, while μ_2 adjusts the balance between information gain and its associated energy cost. Both weights were optimized using Bayesian optimization [32]. Preliminary results suggest that moderate values within these ranges yield a good balance between reliability and energy efficiency.

A. Performance Comparison

In Fig. 7, we show the average information received by the BS per event, which increases with the density of IoTds. This is because more IoTds are active at the same time, providing

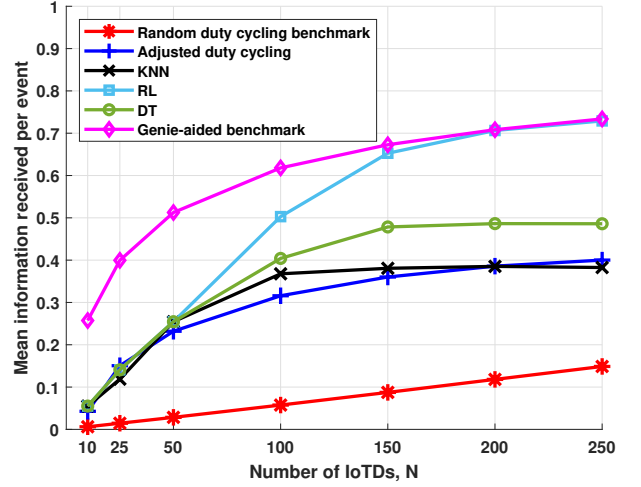


Fig. 7. Mean information received by the BS per event as a function of the number of IoTds.

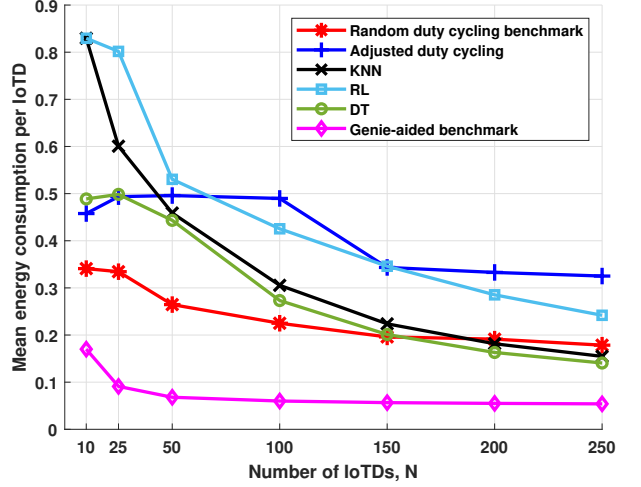


Fig. 8. Mean energy consumption per IoTd per TTI as a function of the number of IoTds.

more information to the BS. Herein, the proposed methods consistently outperform the random duty cycling benchmark, regardless of the IoTds density. Specifically, the adjusted duty cycling and the KNN-based proposals can provide up to ~ 0.4 units of information per event while the RL-based solution approaches the performance of the genie-aided benchmark for high-density scenarios with ~ 0.72 units of information per event. Note that with the genie-aided method, the BS always obtains the greatest amount of information from the event. Similarly, the DT-based proposal outperforms the other methods and the random duty cycling benchmark. However, its performance still falls significantly short compared to the RL-based solution and the genie-aided benchmark. On the other hand, for low-density scenarios $N \leq 50$, all proposed methods have similar performance, outperforming the random duty cycling benchmark but without approaching the optimal values given by the genie-aided benchmark.

Hereinafter, we also investigate the mean energy consumption per device per TTI as the density of IoTds increases. The results depicted in Fig. 8 show that for a setup with 10 IoTds the mean energy consumption for the proposals is around 0.45-0.83 units per IoTd per TTI and only 0.34 units for the random duty cycling benchmark due to its poor event-detection

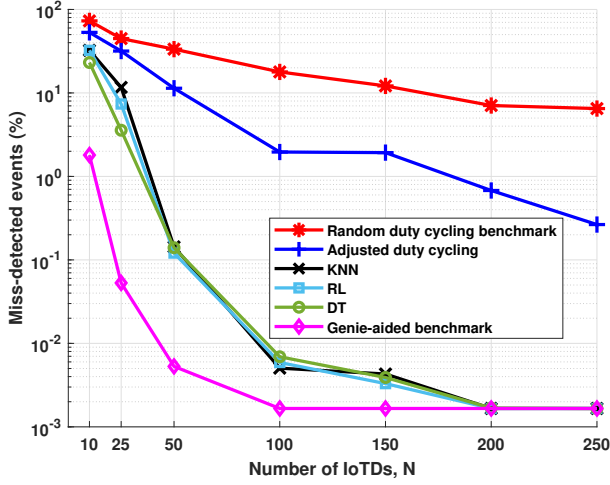


Fig. 9. Percentage of misdetections as a function of the number of IoTs.

performance. As the device density increases, the mean energy consumption decreases up to 0.145 units for the proposed KNN-based method. In contrast, the mean energy consumption for the random duty cycling benchmark is above 0.18 units per TTI, which means that energy consumption increases by more than 29%. Meanwhile, the proposed RL-based solution and the adjusted duty cycling decrease the energy consumption down to 0.24 and 0.32 units, respectively. Notably, for more than 180 IoTs, the mean energy consumption of the proposed KNN-based method is lower than for the random duty cycling benchmark. In addition, Fig. 8 shows how the mean energy consumption per device per TTI decreases 40% and 10% when using the DT-based proposal compared to the initial RL-based and the KNN-based methods, respectively. As the deployment density increases, the proposed methods reduce the gap in energy consumption regarding the genie-aided benchmark. In high density scenarios, this can result in a reduction of up to 0.145 units per IoT per TTI, compared to 0.055 units per IoT with the genie-aided approach.

In Fig. 9, we illustrate the probability of misdetection for each configuration as a function of the IoTs deployment density. As expected, the probability of misdetection decreases with the density. For instance, the misdetection probability is around 33%, 58%, and 77% for the KNN-based approach, adjusted duty cycling approach, and random duty cycling benchmark, respectively, when $N = 10$, thus evincing many/large blind spots. However, as the IoT density increases, the probability drops below 0.01% for the proposed KNN-based and RL-based solutions. For the random duty cycling benchmark, the misdetection probability drops to a minimum of 7% for deployments with 250 IoTs. Notice that the KNN-based, RL-based, and DT-based solutions outperform both the adjusted duty-cycle proposal and the random duty cycling benchmark. Even though the adjusted duty cycling can outperform the benchmark by up to a 200%, just optimizing the duty cycling is not enough to lower the misdetection probability below 2% for deployments with less than 200 IoTs. Note that with the genie-aided approach, the probability of misdetection drops from 2% to near 0.003% as the IoT density increases. This is because IoTs have higher energy availability, as they do

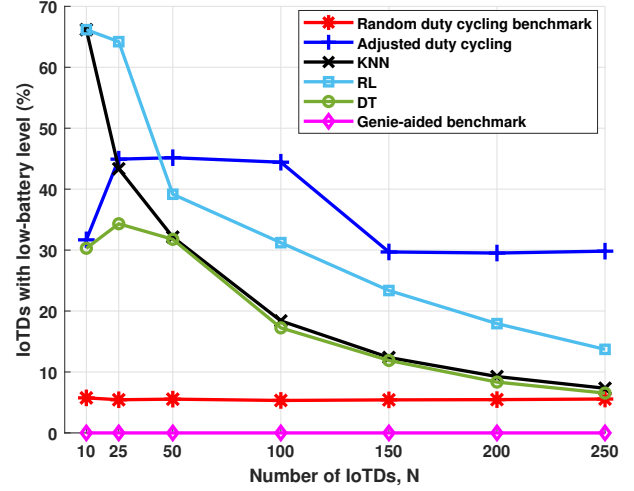


Fig. 10. Percentage of IoTs with low-energy availability to Tx ($B < E_{Tx}$) per TTI as a function of the number of IoTs.

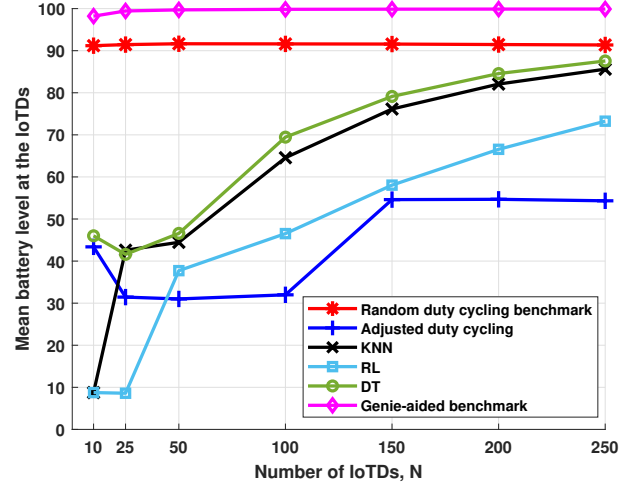


Fig. 11. Mean battery level per TTI as a function of the number of IoTs.

not waste energy on sensing while there is no event happening. However, there is still a small probability that the IoT that detected the event does not have enough energy to transmit. This value, which is $\sim 0.001\%$, is independent of the number of IoTs and constitutes a lower bound.

Figs. 10 and 11 show the mean number of IoTs with low-energy availability per TTI and the mean battery level of the IoTs per TTI. These capture the IoT availability for sensing and transmission. These performance metrics stay around the same level for both the random duty cycling and the genie-aided benchmarks. Meanwhile, the mean number of IoTs with low-energy availability decreases with the device density for the KNN-based and RL-based proposals from around 67% for 10 IoTs to 8%-13% for 250 IoTs. Similarly, the mean IoT battery level per TTI increases from around 10 units to 72-86 units in high-density scenarios. For the optimized duty cycling proposal, the number of devices with low-energy availability fluctuates around 30% - 45% while the mean battery level is around 31-54 units. Moreover, for the proposal based on DT, the IoTs with low energy availability also decrease in a 50%, and the mean battery is always above 40 units per IoT, increasing to almost 88 units per IoT for high-density scenarios.

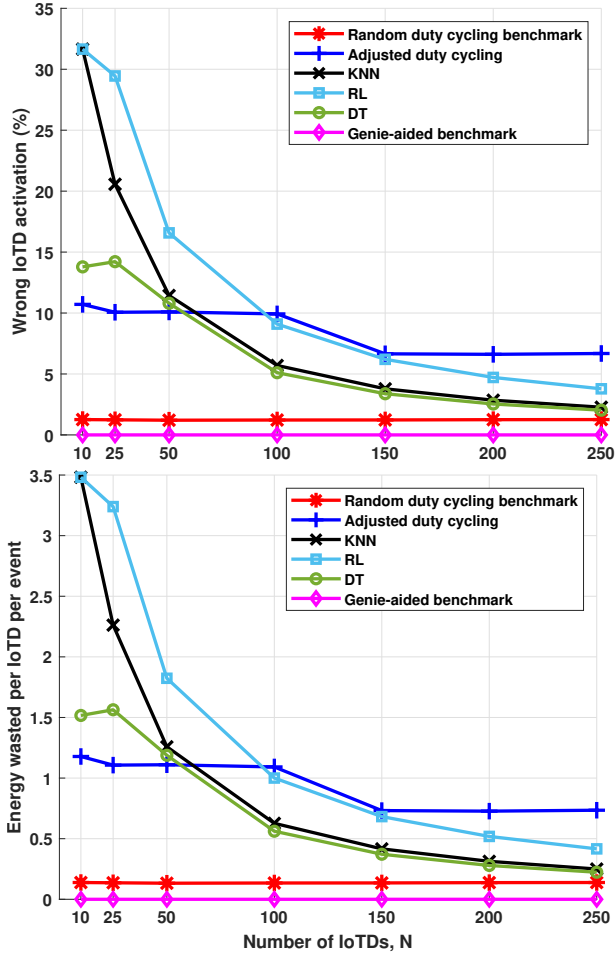


Fig. 12. a) Wrong IoT activation due to low-energy availability or event out of range (top), and b) the corresponding wasted energy as a function of the number of IoTs (bottom).

Next, we analyze how many IoTs are activated wrongly per event. This occurs when the activated IoTs have low-energy availability and thus cannot transmit (failure) or when the BS wakes-up IoTs far from the event epicenter. Fig. 12a shows this wrong activation of IoTs while the corresponding energy level wasted due to the previous situations is shown in Fig. 12b. The genie-aided benchmark does not waste any energy since it always makes the best decision at first. Note that the energy wasted per IoT decreases with the device density, but also more wrong activations occur. Notably, the optimized duty cycling leads to around 17 wrong activations per event for high-density scenarios while the RL-based proposal leads to 9.5 wrong IoT activations pursuing a higher amount of information per event while the KNN-based proposal leads to less than 6 wrong activation. Using the DT-based proposal, the number of wrong IoTs activations per event decreases by 50%, outperforming the other proposed methods and lowering the energy wasted per event below 1.5 units per IoT despite the device density, as shown in Fig. 12b).

Note that the proposed KNN-based and RL-based methods run on the BS, and the cost for the IoTs is negligible. Moreover, the KNN-based proposal can be performed offline given the spatial information of the IoTs.

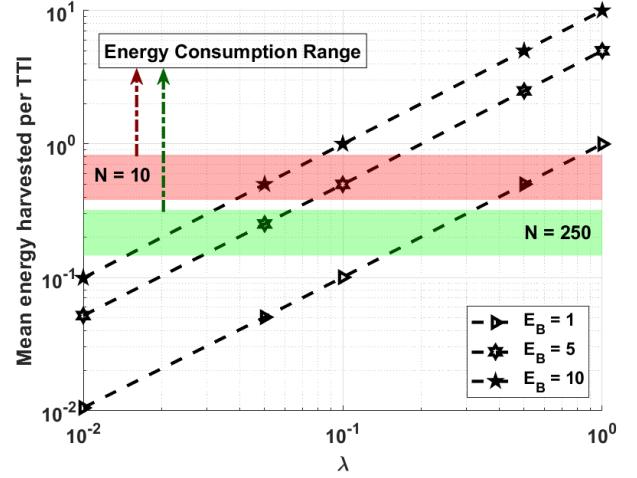


Fig. 13. Mean energy units harvested per IoT per TTI as a function of the EH rate (λ) for $E_B \in \{1, 5, 10\}$ energy units. Light red and green areas show the mean energy consumption when using the benchmark and proposals for $N = 10$ and $N = 250$ respectively. Upper and lower bounds of the regions correspond respectively to the proposed RL and random benchmark methods for $N = 10$ and adjusted duty cycling and DT methods for $N = 250$.

B. EH Analysis

The parameter λ has a significant impact on the likelihood of the energy source being active within a TTI. A good understanding of λ is crucial for efficient energy management in IoT systems, particularly those relying on EH. Fig. 13 depicts the average energy units harvested per IoT per TTI as the parameter λ varies. The red region indicates the energy consumption range for the scenario with $N = 10$, while the green region corresponds to $N = 250$. Specifically, the upper/lower bounds of the red (green) regions correspond to the energy consumption when using the RL-based proposal/random duty cycling benchmark (adjusted duty cycling/DT-based proposal), as shown in Fig. 8. It is important to note that when the IoTs can harvest just one energy unit per energy arrival, the energy consumption is lower than the energy arrival per TTI when using the benchmark and proposals for λ above 0.15-0.3 in high-density scenarios, whereas, for low-density scenarios, this increases to 0.4-0.9. In the case of 5 and 10 energy units per energy arrival, λ could be as low as 0.05 and 0.02, respectively, for high-density scenarios, while for low-density scenarios, it increases to 0.09 and 0.05, respectively.

Moreover, Fig. 14 illustrates the net energy harvested per IoT per TTI as λ varies. The curves represent the methods with the most/least energy consumption adjusted duty cycling/random benchmark for $N = 100$, as shown in Fig. 8. We calculate the net energy harvested as the difference between the mean energy harvested and the energy consumption. Note that when IoTs can harvest just one energy unit per energy arrival, the net energy harvested is positive for $\lambda > 0.38$ and $\lambda > 0.23$ for the upper/lower energy consumption bound, respectively. In the case of 5 and 10 energy units per energy arrival, λ could be as low as 0.052/0.096 and 0.023/0.048, for the upper/lower bound, respectively.

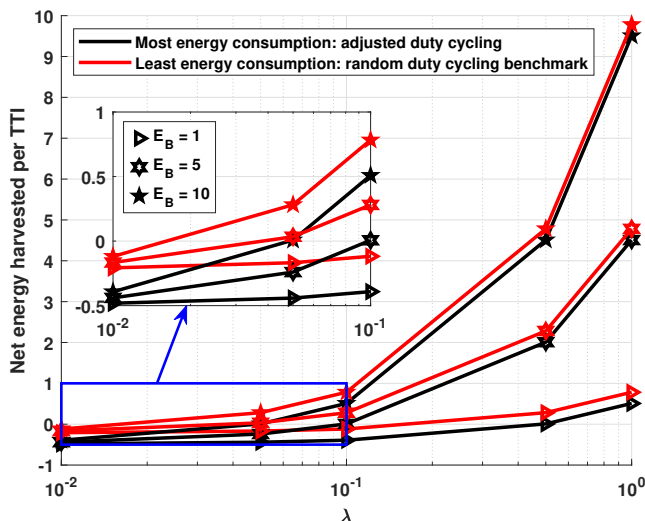


Fig. 14. Mean net energy units harvested per IoT per TTI as a function of the energy arrival rate (λ) for $E_B \in \{1, 5, 10\}$ energy units. The curves represent the upper/lower energy consumption bounds, which correspond to adjusted duty cycling/random benchmark for $N = 100$.

VII. CONCLUSIONS

Energy-efficient strategies and optimized resource allocation are vital for the sustainability of IoT networks, especially those powered by EH. This work focused on an EH-driven IoT system for event monitoring, where IoT devices operate solely on harvested energy. IoT behavior is modeled using a four-state Markov chain for sensing and sleep transitions, a modulated Poisson process for EH dynamics, and a discrete-time Markov chain for battery evolution. We proposed a spatially aware KNN-based duty cycling combined with WuR to reduce energy consumption while preserving detection accuracy. Additionally, RL and DT-based methods are introduced to maximize event-related information collection under energy constraints. Compared to a random duty cycling benchmark, our methods improve information received per event by up to 4.5 times and reduce energy use by up to 23%, approaching the performance of an ideal genie-aided benchmark. These results highlight the effectiveness of combining spatial correlation-aware heuristics with ML for self-sustainable EH-IoT networks. Future work will address scalability and adaptive strategies for heterogeneous EH conditions.

REFERENCES

- [1] O. L. López *et al.*, "Energy-Sustainable IoT Connectivity: Vision, Technological Enablers, Challenges, and Future Directions," *IEEE Open J. Commun. Soc.*, vol. 4, pp. 2609–2666, Oct. 2023.
- [2] L. Belli *et al.*, "IoT-enabled smart sustainable cities: Challenges and approaches," *Smart Cities*, vol. 3, no. 3, pp. 1039–1071, Sep. 2020.
- [3] O. López *et al.*, "Zero-energy devices for 6g: Technical enablers at a glance," *IEEE Internet Things Mag.*, vol. 8, no. 3, pp. 14–22, Apr. 2025.
- [4] D. E. Ruiz-Guirola *et al.*, "Energy-Efficient Wake-Up Signalling for Machine-Type Devices Based on Traffic-Aware Long Short-Term Memory Prediction," *IEEE Internet Things J.*, vol. 9, no. 21, pp. 21 620–21 631, Nov. 2022.
- [5] S. Rostami *et al.*, "Novel wake-up scheme for energy-efficient low-latency mobile devices in 5G networks," *IEEE Trans. Mobile Comput.*, vol. 20, no. 4, pp. 1511–1528, Jan. 2020.
- [6] R. O. S. Juan *et al.*, "Development of a sensing module for standing and moving human body using a shutter and PIR sensor," *International J. Multimedia Ubiquitous Eng.*, vol. 11, no. 7, pp. 47–56, Jul. 2016.

- [7] G. Li *et al.*, "The effect of wireless sensor nodes deployment density in forest fire monitoring quality evaluation," *J. Netw.*, vol. 7, no. 7, pp. 1116–1122, Jul. 2012.
- [8] University of Oulu, "Smart Campus Oulu indoor climate, air-quality and motion," <https://doi.org/10.23729/b9adb0a2-7381-45db-b32f-7e78ae1bc9e3>, 6 2021, University of Oulu, CWC - Verkot ja järjestelmät.
- [9] K. Mikhaylov and H. Karvonen, "Wake-up radio enabled BLE wearables: empirical and analytical evaluation of energy efficiency," in *ISMICT Nara, Japan*, May 2020.
- [10] E. V. Belmega *et al.*, "Online convex optimization in wireless networks and beyond: The feedback-performance trade-off," in *IEEE WiOpt*, Torino, Italy, Sept. 2022, pp. 298–305.
- [11] D. E. Ruiz-Guirola *et al.*, "Configuring Transmission Thresholds in IIoT Alarm Scenarios for Energy-Efficient Event Reporting," *IEEE Open J. Commun. Soc.*, vol. 6, pp. 5490–5508, 2025.
- [12] N. Ma *et al.*, "ESCVAD: an energy-saving routing protocol based on Voronoi adaptive clustering for wireless sensor networks," *IEEE Internet Things J.*, vol. 9, no. 11, pp. 9071–9085, Oct. 2021.
- [13] S. ul Haque *et al.*, "Learning to Speak on Behalf of a Group: Medium Access Control for Sending a Shared Message," *IEEE Commun. Lett.*, vol. 26, no. 8, pp. 1843–1847, Aug. 2022.
- [14] P. Raghuvanshi *et al.*, "Channel Scheduling for IoT Access With Spatial Correlation," *IEEE Commun. Lett.*, vol. 28, no. 5, pp. 1014–1018, Feb. 2024.
- [15] F. Benkhelifa *et al.*, "Recycling cellular energy for self-sustainable IoT networks: A spatiotemporal study," *IEEE Trans. Wireless Commun.*, vol. 19, no. 4, pp. 2699–2712, Apr. 2020.
- [16] W. Li *et al.*, "A Survey on Transformers in Reinforcement Learning," *Trans. Mach. Learning Research*, Sep. 2023. [Online]. Available: <https://openreview.net/forum?id=r30yuDPvf2>
- [17] S. Hu *et al.*, "On Transforming Reinforcement Learning With Transformers: The Development Trajectory," *IEEE Trans. Pattern Anal. Mach. Intell.*, vol. 46, no. 12, pp. 8580–8599, Jun. 2024.
- [18] F. E. Salem *et al.*, "Traffic-aware advanced sleep modes management in 5G networks," in *IEEE WCNC*, Marrakesh, Morocco, Apr. 2019.
- [19] J. Managré and N. Khatri, "A Review on IoT and ML Enabled Smart Grid for Futurestic and Sustainable Energy Management," in *ICONAT*, Goa, India, Jan. 2022.
- [20] S. U. Minhaj *et al.*, "Intelligent Resource Allocation in LoRaWAN Using Machine Learning Techniques," *IEEE Access*, vol. 11, pp. 10 092–10 106, Jan. 2023.
- [21] S. Shabana Anjum *et al.*, "Energy optimization of sustainable Internet of Things (IoT) systems using an energy harvesting medium access protocol," in *IOP Conference Series: Earth and Environmental Sci.*, vol. 268, no. 1. IOP Publishing, 2019, p. 012094.
- [22] K. Nadali *et al.*, "Machine-Learning-Based Predictive Modeling Analysis in Ambient RF Energy Harvesting for IoT Systems," *IEEE Sensors J.*, vol. 24, no. 2, pp. 2242–2254, Nov. 2023.
- [23] D. E. Ruiz-Guirola *et al.*, "Intelligent Duty Cycling Management and Wake-up for Energy Harvesting IoT Networks with Correlated Activity," in *58th Asilomar Conference Signals, Syst. Computers*, Oct. 2024.
- [24] V. Egorova *et al.*, "Computation of the regularized incomplete Beta function," *DRNA*, vol. 16, no. 16.3, pp. 10–16, Jul. 2023.
- [25] M. A. Wiering and M. Van Otterlo, "Reinforcement learning," *Adaptation, Learning, and Optimization*, vol. 12, no. 3, pp. 3–42, Mar. 2012.
- [26] S. Lu *et al.*, "Deep Reinforcement Learning-Based Intelligent Reflecting Surface for cooperative Jamming Model Design," *IEEE Access*, vol. 11, pp. 98 764–98 775, Sep. 2023.
- [27] A. Vaswani *et al.*, "Attention is all you need," *Proc. NIPS, California, USA*, vol. 30, Dec. 2017.
- [28] D. Zhu *et al.*, "Efficient precision-adjustable architecture for softmax function in deep learning," *IEEE Trans. Circuits Syst. II*, vol. 67, no. 12, pp. 3382–3386, Jun. 2020.
- [29] H. Thomsen *et al.*, "A traffic model for machine-type communications using spatial point processes," in *IEEE PIMRC*, Montreal, QC, Canada, Oct. 2017.
- [30] I. Howitt *et al.*, "Extended energy model for the low rate WPAN," in *IEEE Conference Mobile Adhoc Sensor Syst.*, Washington, DC, Nov. 2005.
- [31] S. Fowler *et al.*, "Analysis of adjustable and fixed DRX mechanism for power saving in LTE/LTE-Advanced," in *IEEE ICC*, Ottawa, ON, Canada, Jun. 2012, pp. 1964–1969.
- [32] R. Garnett, *Bayesian optimization*. Cambridge University Press, United Kingdom, Feb. 2023.